

## Article

# Surface Morphology and Mechanical Properties of Polyether Ether Ketone (PEEK) Nanocomposites Reinforced by Nano-Sized Silica (SiO<sub>2</sub>) for Prosthodontics and Restorative Dentistry

Ahmed Abd El-Fattah <sup>1,2,\*</sup>, Heba Youssef <sup>3</sup>, Mohamed Abdel Hady Gepreel <sup>4</sup> , Rafik Abbas <sup>1</sup> and Sherif Kandil <sup>1</sup>

<sup>1</sup> Department of Materials Science, Institute of Graduate Studies and Research, Alexandria University, El-Shatby, Alexandria 21526, Egypt; rafik.abbas@yahoo.com (R.A.); s.kandil@usa.net (S.K.)

<sup>2</sup> Department of Chemistry, College of Science, University of Bahrain, Sakhir P.O. Box 32038, Bahrain

<sup>3</sup> College of Dentistry, Arab Academy for Science, Technology and Maritime Transport (AASTMT), El-Alamein 51718, Egypt; heba.youssef@aast.edu

<sup>4</sup> Department of Materials Science and Engineering, Egypt-Japan University of Science and Technology (E-JUST), New Borg El-Arab City 21934, Egypt; gepreel@yahoo.com

\* Correspondence: a\_abdelfattah@alexu.edu.eg or aahusseini@uob.edu.bh



**Citation:** Abd El-Fattah, A.; Youssef, H.; Gepreel, M.A.H.; Abbas, R.; Kandil, S. Surface Morphology and Mechanical Properties of Polyether Ether Ketone (PEEK) Nanocomposites Reinforced by Nano-Sized Silica (SiO<sub>2</sub>) for Prosthodontics and Restorative Dentistry. *Polymers* **2021**, *13*, 3006. <https://doi.org/10.3390/polym13173006>

Academic Editor: Ivan Guryanov

Received: 24 July 2021

Accepted: 30 August 2021

Published: 5 September 2021

**Publisher's Note:** MDPI stays neutral with regard to jurisdictional claims in published maps and institutional affiliations.



**Copyright:** © 2021 by the authors. Licensee MDPI, Basel, Switzerland. This article is an open access article distributed under the terms and conditions of the Creative Commons Attribution (CC BY) license (<https://creativecommons.org/licenses/by/4.0/>).

**Abstract:** In the field of orthopedics and traumatology, polyether ether ketone (PEEK) serves a significant role as a suitable alternative to traditional metal-based implants like titanium. PEEK is being used more commonly to replace traditional dental products. For bonding with various adhesive agents and preserved teeth, the surface alteration of PEEK was investigated. The aim of this research was to understand how different types and contents of nano-sized silica (SiO<sub>2</sub>) fillers influenced the surface and mechanical properties of PEEK nanocomposites used in prosthodontics. In this work, PEEK based nanocomposites containing hydrophilic or hydrophobic nano-silica were prepared by a compression molding technique. The influence of nano-SiO<sub>2</sub> type and content (10, 20 and 30% wt) on surface properties of the resultant nanocomposites was investigated by the use of scanning electron microscopy (SEM), energy-dispersive X-ray spectroscopy (EDX), surface roughness analysis, and contact angle measurement. The crystalline structures of PEEK/SiO<sub>2</sub> nanocomposites were examined by X-ray diffraction (XRD) spectroscopy. Mechanical properties were measured by microhardness, elastic compression modulus, and flexural strength. All nanocomposites showed increased surface roughness compared to pure PEEK. SEM images revealed that nanocomposites filled with low content hydrophobic nano-SiO<sub>2</sub> showed uniform dispersion within the PEEK matrix. The introduction of 10 wt% of hydrophobic nano-SiO<sub>2</sub> to the PEEK matrix improved elastic modulus, flexural strength, and microhardness, according to the findings. The addition of nano-SiO<sub>2</sub> fillers in a higher weight percentage, over 10%, significantly damages the mechanical characteristics of the resultant nanocomposite. On the basis of the obtained results, PEEK/SiO<sub>2</sub> nanocomposites loaded with low content hydrophobic nano-SiO<sub>2</sub> are recommended as promising candidates for orthopedic and prosthodontics materials.

**Keywords:** PEEK; nano-silica; nanocomposites; prosthodontics; surface properties; elastic modulus; microhardness; flexural strength; compression molding

## 1. Introduction

Prosthodontics is a major branch of dental medicine. It has become the main driver of dental treatment and the centerpiece of dental science with the rise of human welfare, standard of living, and the increased level of oral health awareness. Prosthodontics mostly manages dental defects and rehabilitation after tooth loss (such as crowns, dentures and lays), as well as extending the uses of artificial prostheses for periodontal disease, temporomandibular joint disease, and maxillofacial tissue defects [1,2]. Prosthodontic dental

materials can be classified into three categories: metals, ceramics and resins. The qualities of these materials are important in the construction of dental prostheses, which are in direct contact with the oral mucosa and under long-term use in the oral environment. Therefore, the dental materials must have comprehensive properties and good biological activity to function properly [3–5].

Dental materials should have high mechanical strength, toughness, higher fatigue strength, high elastic modulus, low thermal and electrical conductivity, good castability, and low shrinkage deformation. Chemical stability is also needed, such as resistance to corrosion, breakage, and the effects of aging. The colors of dental materials can be formulated and should keep long-term stability. A good oral material should have adequate biocompatibility and safety, and be biofunctional [6–8]. However, due to the nature of the material itself, its continued use for long period in moist environment, a variety of problems, such as pigment coalescence, color change, and aging fractures, do occur [9,10].

In recent years, advances in nanomaterials and technology have captured increased attention because of their unique structures and properties. Development of nanomaterials has strengthened many applications in medicine and dentistry [11–13]. Polymeric nanocomposites are a class of nanomaterials in which nanoscale particulates such as spherical inorganic minerals are dispersed within polymeric matrices [14–17]. Compared to pure polymers, polymeric nanocomposites are claimed to show markedly improved properties, such as modulus, strength, dimensional stability, electrical conductivity, barrier performance, solvent resistance, biocompatibility, low plaque affinity, good aesthetics, and characteristics close to dental structure depending on type and content of the nanofiller particles used [18,19].

Polyether ether ketone (PEEK) is an emerging kind of thermoplastic engineering plastic [20]. Modifications and alterations of PEEK have been extensively studied thanks to its wide range of applications in the areas of selective laser sintering, dehumidification, nanofiltration membranes, fuel cells, and biomedical devices [21–24]. PEEK is a semi-crystalline colorless polymer with outstanding mechanical and thermal properties. Excellent thermal stability PEEK materials have a melting point ( $T_m$ ) of 343 °C and a glass transition temperature ( $T_g$ ) of 143 °C. PEEK can be processed using a variety of commercial techniques, including injection molding, extrusion molding, compression molding, and additive manufacturing at temperatures between 350 and 420 °C. Moreover, PEEK is nontoxic, and its sterilization efficiency is excellent. It can be repeatedly sterilized using conventional methods such as those employing steam, gamma radiation, and ethylene oxide, without evident degradation of the mechanical properties [25].

PEEK possesses particularly high durability and firmness, mainly in terms of fatigue and its strength, which is equivalent to alloy constituents [26]. One of the important characteristics of PEEK is its reduced elastic modulus, which ranges between 2 and 6 GPa and efficiently prevents the pressure sheltering influence [27]. Since its elastic modulus is much more related to that of compact skeletal mass, PEEK has emerged as an operational and suitable substitute to traditional implantation such as titanium in the fields of orthopedics [28] and traumatology [29]. PEEK has also been intended for prosthodontic use to produce prosthetic infrastructures and abutments for titanium-based implant systems. However, in those cases, it is essential that the material exhibits high mechanical strength, wear resistance and aesthetic features compatible with those of tooth tissues.

Considerable research interest has recently been directed toward developing PEEK nanocomposite biomaterials to improve various physical, mechanical and barrier properties to allow their application to restorative dentistry [30]. This could be achieved by the incorporation of spherical inorganic nanoparticles, such as nano silica ( $\text{SiO}_2$ ), into the PEEK matrix [31].

Bare  $\text{SiO}_2$  is characterized by its small particle size and large surface area. The surface of silica has three chemical groups of isolated hydroxy, hydrogen-bonded hydroxy, and siloxane groups. Thus, the surface is usually hydrophilic, even though the siloxane groups are hydrophobic. The hydrophilic surface of bare  $\text{SiO}_2$ , however, can be rendered

hydrophobic by reacting its surface hydroxyl groups with organofunctional groups, such as polydimethylsiloxane, dimethyldichlorosilane, and hexamethyldisilane [20].

Compression molding has been used to successfully fabricate PEEK composites reinforced with SiO<sub>2</sub> nanofillers for industrial processes [32]. However, research into SiO<sub>2</sub> nanofillers as PEEK reinforcement in the dental field is minimal.

Several researchers have examined whether surface pre-treatments would enhance the bond strength between PEEK and dental materials [33–35]. In fact, in dental therapy, pre-treatment with a silane binding agent significantly helps in achieving a reliable bond between an inorganic filler-filled dental prosthesis and resin cement [36]. The effect of SiO<sub>2</sub> in PEEK on its bearing capacity to resin cement was investigated in an analysis. The results of that research analysis discovered that increasing the SiO<sub>2</sub> content in PEEK improved the tensile bond strength [37]. As a result, further research is required to fully understand the influence of nanofiller particle form, structure, particle size, total volume, and coating in PEEK for dental applications.

The goal of the present research is to assess the influence of hydrophilic and hydrophobic nano-SiO<sub>2</sub> fillers on the surface and mechanical properties of PEEK nanocomposites for prosthodontics and restorative dentistry, due to the lack of data on PEEK/SiO<sub>2</sub> nanocomposite performance for dental applications.

## 2. Materials and Methods or Experimental

### 2.1. Materials

Semi-crystalline PEEK fine powder (VICTREX<sup>®</sup> PEEK polymers, Victrex Technology Centre, Lancashire FY5 4QD, UK.) with average particle size 50 µm for compression molding was used as the polymer matrix. The density of PEEK is 1.3 g/cm<sup>3</sup>, and its melt viscosity is 350 Pa.s. Two types of amorphous nano-SiO<sub>2</sub> particles (NanoTech Egypt Co., Giza, Egypt) were used as filler materials. The bare hydrophilic nano-SiO<sub>2</sub> had an average particle size of 29 ± 4 nm, while the chemically modified hydrophobic nano-SiO<sub>2</sub> (treated with trimethyl chlorosilane) had an average particle size of 14.5 ± 5 nm.

### 2.2. Preparation of PEEK/SiO<sub>2</sub> Nanocomposites

Prior to mixing, PEEK powder and nano-SiO<sub>2</sub> particles were dried overnight in a vacuum oven at 120 °C to guarantee sufficient elimination of moisture. Then they were ball-milled mixed in a planetary ball mill (Emax, Retsch GmbH, Haan, Germany) at 25 °C and 400 rpm for 2 h. The PEEK/SiO<sub>2</sub> nanocomposites were fabricated using a compression molding process. The as-milled dried powder was filled in tool steel die with 10 mm diameter. The powder was compressed at room temperature under a pressure of 35 MPa for 2 min. After cold compaction, the powder was heated to 410 °C, while applying a low cavity pressure of about 2 MPa. Once the system reached the set temperature, it was held at constant temperature and pressure for 10 min to establish homogeneity within the melt. Following this, the system was permitted to cool down to room temperature under a pressure of 20 MPa. Finally, the mold was opened and the samples were taken out. Custom-designed mold tooling was used to produce the samples for mechanical testing. Table 1 illustrates the precise composition of the prepared PEEK/SiO<sub>2</sub> nanocomposites used in this analysis. PK was used to identify PEEK polymers in this study. Hydrophobic and hydrophilic nano-SiO<sub>2</sub> particles were assigned the codes BS and LS, respectively, followed by a number indicating the weight percentage of nano-SiO<sub>2</sub> particles. For example, the PEEK/SiO<sub>2</sub> nanocomposite with 10 wt% hydrophobic nano-SiO<sub>2</sub> particles, was coded as PKBS-10.

**Table 1.** PEEK/SiO<sub>2</sub> nanocomposites formulations (percentage by weight).

Code	Sample	Silica Content		
		PEEK (wt%)	BS (wt%)	LS (wt%)
PK	Unfilled PEEK	100	0	0
PKBS-10	PEEK/BS 10 wt%	90	10	0
PKBS-20	PEEK/BS 20 wt%	80	20	0
PKBS-30	PEEK/BS 30 wt%	70	30	0
PKLS-10	PEEK/LS 10 wt%	90	0	10
PKLS-20	PEEK/LS 20 wt%	80	0	20
PKLS-30	PEEK/LS 30 wt%	70	0	30

### 2.3. Characterization Methods

#### 2.3.1. X-ray Diffraction (XRD)

Crystal structural analyses of the pure PEEK and PEEK/SiO<sub>2</sub> nanocomposites were performed by powder XRD measurements using a diffractometer (XRD-7000, Shimadzu, Japan). The X-ray beam was Cu-K $\alpha$  radiation ( $\lambda = 0.1542$  nm), operated at 40 kV and 30 mA. The XRD pattern was recorded in the  $2\theta$  range from 10° to 50° with a scanning rate of 5° per min. The crystalline phase was identified and compared to the literature as well as the International Center for Diffraction Data (ICDD) for PEEK.

#### 2.3.2. Scanning Electron Microscopy (SEM)

A scanning electron microscope (SEM) was used to assess the surface morphology of the desired samples. For this purpose, SEM uses a JEOL instrument (JSM-5300, Tokyo, Japan) which was operated at 25 keV. Prior to SEM imaging, the samples were ultrasonically washed for 30 s and sputter-coated with gold to a thickness of 400 Å in a sputter-coating device (JFC 1100 E).

#### 2.3.3. Energy-Dispersive X-ray Spectroscopy (EDX)

The presence of silica on each nanocomposite surface was determined by energy dispersive X-ray (EDX) microanalysis attached to the SEM. Analysis was performed on uncoated samples at 15 kV for 60 s.

#### 2.3.4. Surface Roughness Analyses

The surface roughness (Ra) of the desired samples was examined by an optical profilometer (MarSurf PS1, Mahr GmbH Göttingen, Germany). Four different locations perpendicular to the surface on each sample were recorded. Mean Ra values were statistically analyzed and used as the final Ra score for each sample.

#### 2.3.5. Contact Angle Measurement

Water contact angle experiments in a goniometer digital (RAMÉ-hart Model 190-F2, Succasunna, NJ 07876, USA) had been used to determine the surface hydrophilicity of the samples. The static sessile drop technique was performed using the video contact angle method. To measure the average contact angle and standard deviation, at least seven stabilized contact angles from different sites in each sample were obtained.

#### 2.3.6. Microhardness Measurement

Microhardness of the samples was measured as Vickers hardness number (VHN) (Wolpert micro-Vickers tester, Wolpert Wilson Instruments, division of Instron Deutschland GmbH, Aachen, Germany). The indentations were made using a diamond pyramid micro-indenter with a 136° angle between the opposing faces under a load of 200 N applied for a dwell time of 10 s.

### 2.3.7. Mechanical Tests

Compression analysis was carried out by using a universal testing machine (AG-IS 100KN, Shimadzu Corporation, Kyoto, Kyoto Prefecture, Japan). The test was performed with a cylindrical sample of dimensions (10 mm diameter  $\times$  6 mm height) at a crosshead speed of 1.0 mm/min until the specimen failed. Flexural properties were measured using a three-point bending test method in the same universal testing machine. The test was carried out with a rectangular bar sample of dimension (80 mm  $\times$  6 mm  $\times$  6 mm) at a crosshead speed of 1.0 mm/min at room temperature. A total of seven cases were analyzed for each sample at room temperature. Seven samples were tested for each material group (PEEK, PKBS or PKLS) to obtain the average value.

### 2.4. Statistical Analysis

Statistical Package for the Social Sciences (SPSS) software was used to analyze the results (IBM Corp.: Armonk, NY, US). The Kolmogorov–Smirnov (K–S) test was used to conduct parametric tests, and the results showed that the data were normally distributed. Multiple comparison analyses were performed using variance (ANOVA) analysis with  $p = 0.05$ , Tukey post hoc test, and Student's  $t$ -test.

## 3. Results and Discussion

### 3.1. Fabrication of Nanocomposites

PEEK/SiO<sub>2</sub> nanocomposites were successfully fabricated by dry mixing of PEEK (polymer matrix) and diverse nano-SiO<sub>2</sub> particles (inorganic nanofiller) using high energy ball milling followed by a compression molding process. Ball milling technique was used to disperse nano-SiO<sub>2</sub> particles into the PEEK matrix due to the excellent deformability of thermoplastic polymers. In addition, ball milling was shown to improve the mechanical properties of the polymer by reducing the particle size of pure PEEK from a millimeter to a micrometer scale (~5  $\mu$ m). It is well known that PEEK has a good resistance to most organic solvents except concentrated sulfuric acid (95–98%) and methyl sulfonic acid [37]. As a result of the poor solubility of the PEEK in organic solvents, it is more feasible to fabricate its nanocomposites through the compression molding technique.

In this work, the number of nano-SiO<sub>2</sub> particles was varied at 10%, 20% and 30%. These values were selected because they represent an optimum performance of mechanical properties and the quality of interface between the nanoparticles and polymer matrix [28]. Nevertheless, concentrations exceeding the 30% threshold were discounted to avoid the strong repulsion and attraction forces of nano-SiO<sub>2</sub> particles, which in turn may deteriorate the overall mechanical properties of the composite and hinder the adhesion at the interface between the matrix and the nanofillers [37–40].

### 3.2. Structural Analysis

Figure 1 shows the XRD diffraction patterns of the pure PEEK and PEEK/SiO<sub>2</sub> nanocomposites (PKBS and PKLS groups) loaded with diverse nano-SiO<sub>2</sub> contents (10, 20, and 30 wt%). XRD of both hydrophobic and hydrophilic nano-SiO<sub>2</sub> particles did not show any sharp Bragg peaks, except a broad peak between 15° and 25°, signifying that they have an amorphous structure. The pure PEEK and its nanocomposites crystallize mostly in the form of an orthorhombic crystal structure. The pure PEEK exhibits diffraction peak positions ( $2\theta$ ) of about 18.61°, 20.53°, 22.45°, and 28.62°, corresponding to diffraction planes of (110), (111), (200), and (211).

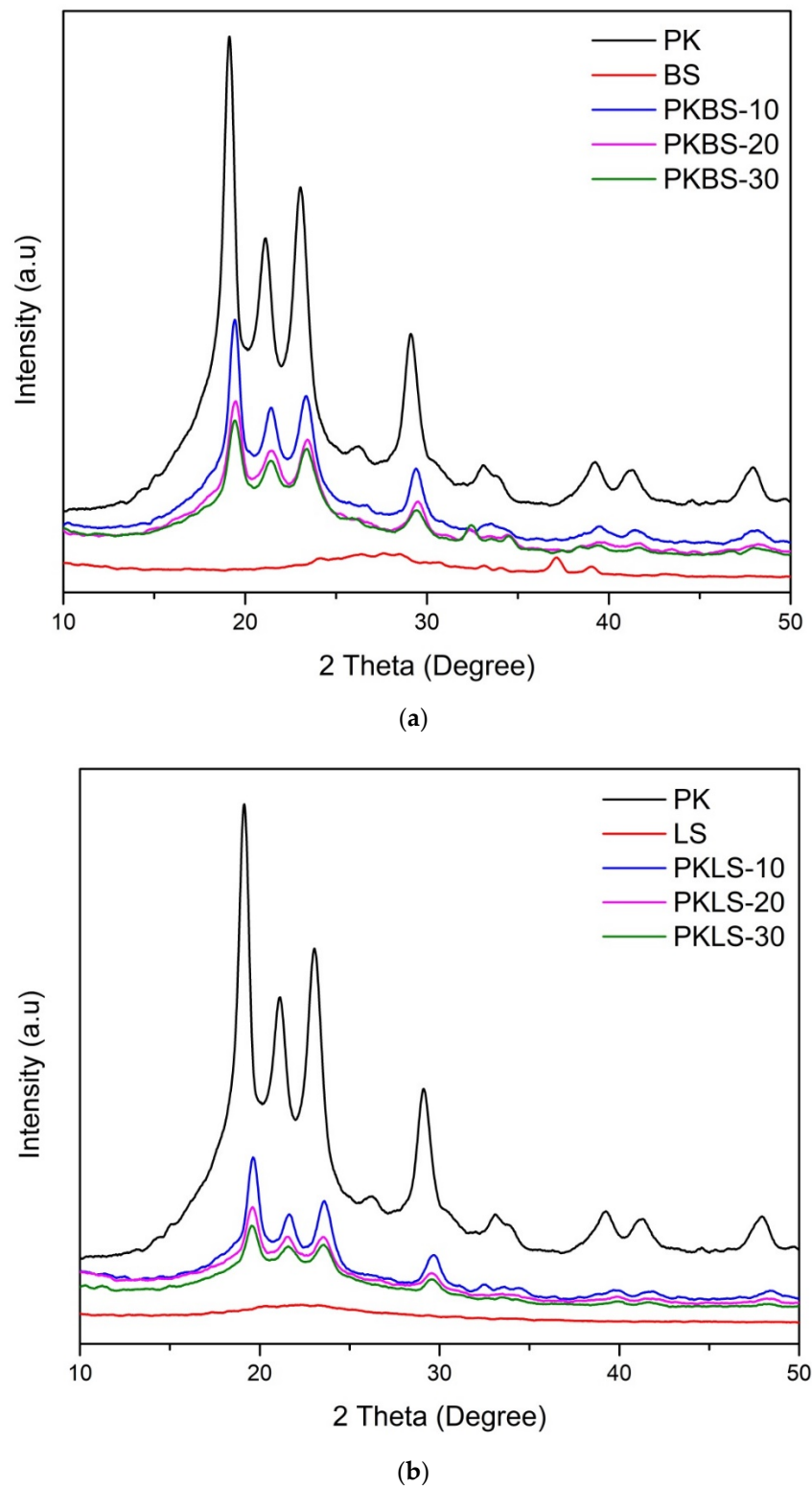


**Figure 1.** XRD patterns showing the effect of the nano-SiO<sub>2</sub> fillers on the crystallinity of PEEK: (a) nanocomposites filled with hydrophobic nano-SiO<sub>2</sub> and (b) nanocomposites filled with hydrophilic nano-SiO<sub>2</sub>.

Evidently, apart from those of pure components, no new diffracting peaks were detected in the diffraction pattern of PEEK/SiO<sub>2</sub> nanocomposites. Moreover, all nanocomposite samples showed the same XRD patterns with decreasing peak intensities in proportion to the nano-SiO<sub>2</sub> content. The results indicated that the increase in both hydrophobic and

hydrophilic nano-SiO<sub>2</sub> content decreases the crystallinity of the PEEK matrix. Similarly, in a previous study conducted on the crystallization behavior of the nano-SiO<sub>2</sub> filled PEEK composites, it was concluded that the inclusion of the 15 nm SiO<sub>2</sub> particles would significantly decrease the crystallinity of the PEEK matrix by about 15% under isothermal crystallization, due to the hindrance of mobility [39]. Experimental evidence indicated that nano-SiO<sub>2</sub> has little effect on the degree of crystallinity and that it does not act as a nucleating agent [40]. It has been shown that, for the given number of nanoparticles, the polymer crystallization was reduced by impeding the arrangement of molecular chains for the formation of the lamellae [37].

### 3.3. Morphological Observation

SEM micrographs of the pure PEEK and PEEK/SiO<sub>2</sub> nanocomposites loaded with different nano-SiO<sub>2</sub> contents (10, 20, and 30 wt%) were captured to examine the exact microstructure as shown in Figure 2. As displayed in Figure 2a, the pure PEEK micrograph revealed a relatively homogenous, smooth, and uniform surface. The effect of incorporation of hydrophobic nano-SiO<sub>2</sub> on the morphology of the nanocomposites is illustrated in Figure 2b–d. The addition of low hydrophobic nano-SiO<sub>2</sub> content (10 wt%) in the nanocomposite showed uniform dispersion within the polymer matrix, leaving a relatively smooth surface (Figure 2b). On the contrary, a clear nano-SiO<sub>2</sub> agglomeration and increased surfaces roughness were observed in the nanocomposites containing high hydrophobic nano-SiO<sub>2</sub> content (30 wt%).

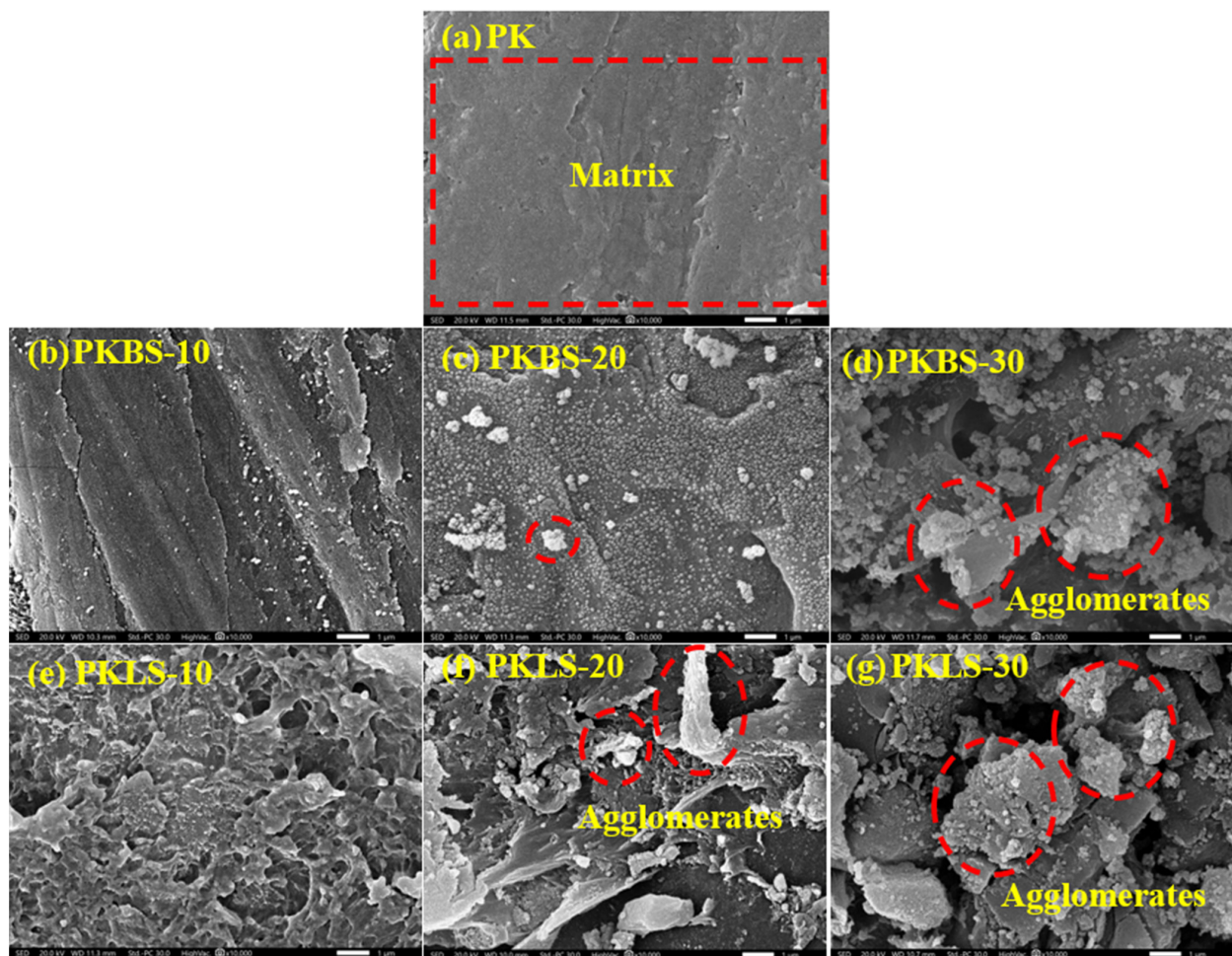


Figure 2. SEM micrographs showing the dispersion of the nano-SiO<sub>2</sub> fillers in the PEEK matrix.

On the other hand, the SEM micrographs of the PEEK/SiO<sub>2</sub> nanocomposites based on different hydrophilic nano-SiO<sub>2</sub> contents (10, 20, and 30 wt%), as presented in Figure 2e,f, exhibited poor dispersibility and weak interfacial adhesion of hydrophilic nano-SiO<sub>2</sub> with the polymer matrix. Moreover, the PEEK/SiO<sub>2</sub> nanocomposites based on hydrophilic nano-SiO<sub>2</sub> (PKLS group) exhibited a rougher surface than their corresponding PEEK/SiO<sub>2</sub> nanocomposites based on hydrophobic nano-SiO<sub>2</sub> (PKBS group) counterparts.

These results might be due to the additions of nano-SiO<sub>2</sub> particles to the PEEK matrix, leading to various nano-SiO<sub>2</sub> particle–particle and nano-SiO<sub>2</sub> particle–PEEK chain interactions, allowing formations of aggregates and agglomerates on the surface of PEEK nanocomposites [20,37]. Such agglomerations are less evident for PEEK/SiO<sub>2</sub> nanocomposites containing hydrophobic nano-SiO<sub>2</sub> particles, causing smoother surfaces compared with PEEK/SiO<sub>2</sub> nanocomposites embedded with hydrophilic nano-SiO<sub>2</sub> particles.

### 3.4. Compatibilization of Hydrophobic Polymer and Nanofiller

The quality of the filler-matrix interface is significant for the application of inorganic filler particles as reinforcing materials in polymer matrices. The properties of nanocomposites depend on all of the individual components and on their compatibility. In general, homogeneous and uniform distribution of nanofiller particles in polymer matrices is extremely crucial for the improvement of physicochemical properties and mechanical characteristics of polymer matrix nanocomposites (PMNCs). Therefore, the poor distribution of nanoparticles in polymer matrices causes potential problems in the fabrication of PMNCs [37,38]. It is generally acknowledged that the aggregation of particles is highly dependent on their dispersion within the polymer matrix. The increase in the degree of particle dispersion results in decreasing particle aggregation.

EDX analysis was conducted to examine the dispersion of nano-SiO<sub>2</sub> on the surface of the PEEK polymer matrix. Figure 3 shows the presence of chemical elements on the surface of pure PEEK as well as on the surface of various PEEK/SiO<sub>2</sub> nanocomposites. In these patterns, there is no Si present on pure PEEK (Figure 3a). EDX analysis of PEEK/SiO<sub>2</sub> nanocomposites containing 10 wt% hydrophobic nano-SiO<sub>2</sub> as presented in Figure 3b illustrates more efficient interactions and higher compatibility between PEEK chains and hydrophobic nano-SiO<sub>2</sub>, leading to a lower presence of Si at these composites' surfaces. However, hydrophilic nano-SiO<sub>2</sub> particles (Figure 3e–g) containing hydroxyl groups have a strong tendency to agglomerate due to their incompatibility with the matrix, leading to migration to the surface of such composites. This finding is also further supported by previous reported data [41,42].

Based on the SEM observations and EDX analysis, a schematic presentation of possible interactions and dispersion of nano-SiO<sub>2</sub> particles in the PEEK matrix is presented in Figure 4. The presence of hydroxyl groups on the surface of hydrophilic nano-SiO<sub>2</sub> particles increases the particles' interactions, through hydrogen bonding, which cause particle aggregation and network formation—potentially adversely influencing the nanoparticles' distribution in the PEEK matrix [20]. In addition, the strength of interfacial interactions between the PEEK and nano-SiO<sub>2</sub> particles is the most determining factor affecting the properties of the obtained nanocomposites. It is possible that hydrophilic nano-SiO<sub>2</sub> particles make interfacial interactions and bond with hydroxyl end groups of PEEK chains. On the other hand, surface chemical modification is one of the various methods to improve the compatibility between the hydrophobic PEEK and hydrophilic nano-SiO<sub>2</sub>. Consequently, a good dispersion may be achieved by using hydrophobic nano-SiO<sub>2</sub>, due to its uniform incorporation within the hydrophobic PEEK matrix.

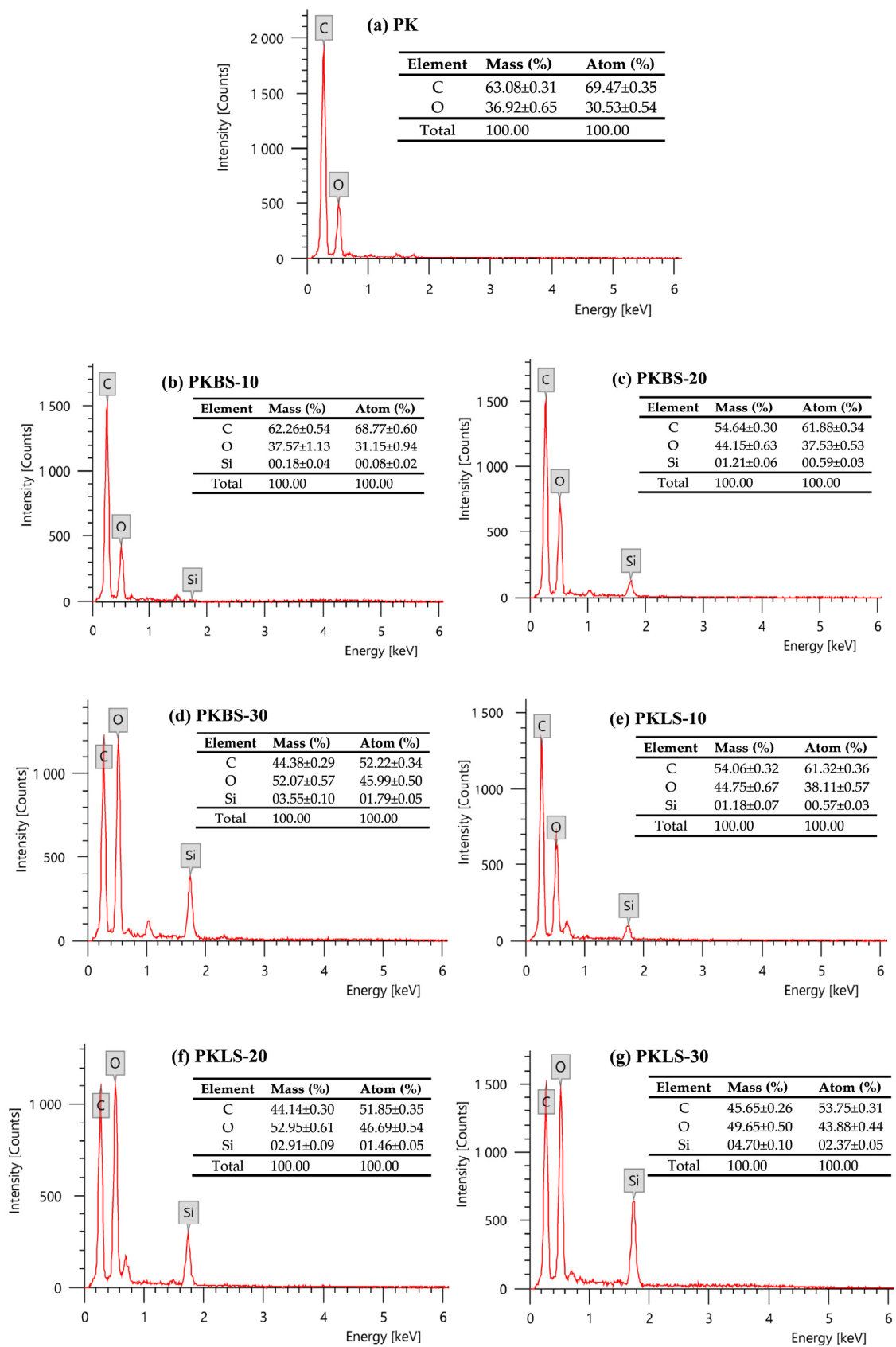
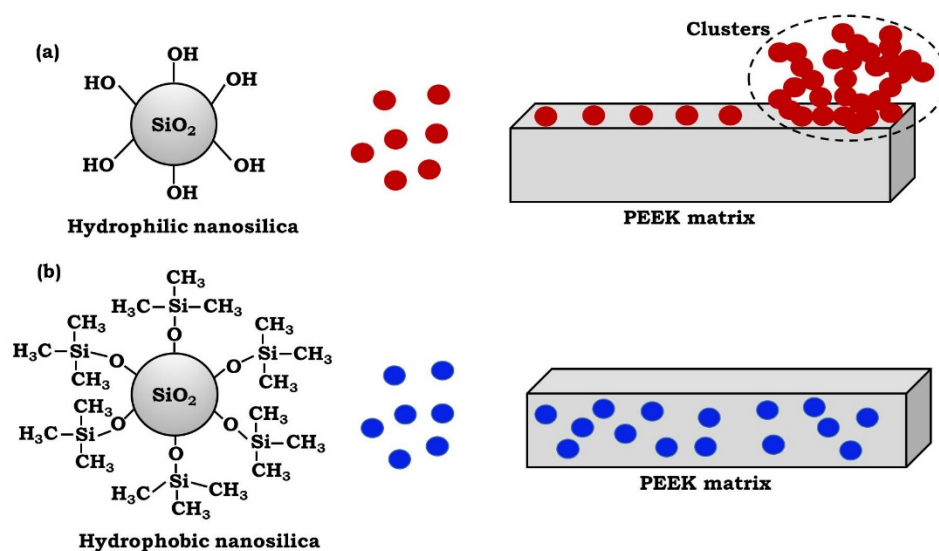


Figure 3. EDX analysis of pure PEEK as well as various PEEK/SiO<sub>2</sub> nanocomposites.



**Figure 4.** Schematic representation of the degree of dispersion and distribution of nano-SiO<sub>2</sub> particles in the PEEK polymer matrix. (a) The hydrophilic nano-SiO<sub>2</sub> particles are fused together into clusters with an irregular, chain-like geometry. (b) The hydrophobic nano-SiO<sub>2</sub> particles exhibit good dispersion and distribution within the hydrophobic PEEK matrix.

### 3.5. Surface Roughness (*R<sub>a</sub>*)

Average values of surface roughness for the pure PEEK and PEEK/SiO<sub>2</sub> nanocomposites loaded with diverse nano-SiO<sub>2</sub> contents (10, 20, and 30 wt%) are summarized in Table 2. The results indicated that the surface roughness values increase with the increase of the nano-SiO<sub>2</sub> contents in the nanocomposites. For example, the addition of 30 wt% hydrophilic nano-SiO<sub>2</sub> markedly increased the surface roughness value of the pure PEEK from 1.43 to 3.32 μm (130%) in the nanocomposite. Furthermore, the roughness values are higher for the PEEK/SiO<sub>2</sub> nanocomposites embedded with hydrophilic nano-SiO<sub>2</sub> particles compared the hydrophobic ones. The approach of using additives to modify surface and bulk properties of performance polymers is well-known [41]. Generally, the ability of additives to migrate to the surface is defined by factors such as particle size, composition, end-group functionalities, molecular architecture, and concentration. Besides, the careful selection of additives with proper functionalities provides significant control over the hydrophilicity or hydrophobicity of modified surfaces while retaining bulk properties [42]. The PEEK and nano-silica particles have some interfacial interactions within the PEEK matrix. However, it appears that these interactions are not strong enough to enable a good dispersion of the hydrophilic nano-SiO<sub>2</sub> particles within the PEEK matrix [43]. The formation of hydrogen bonds between the surface hydroxyl groups of the hydrophilic nano-SiO<sub>2</sub> particles may be responsible for particle aggregation within the matrix [44].

**Table 2.** Mean values and standard deviation (mean ± SD) for surface roughness and contact angle data of pure PEEK together with various PEEK/SiO<sub>2</sub> nanocomposites.

Code	Sample ( <i>n</i> = 7)	Surface Roughness ( <i>R<sub>a</sub></i> ) (μm)	Contact Angle (°)
PK	Unfilled PEEK	1.45 ± 0.35	93.71 ± 1.52
PKBS-10	PEEK/BS 10 wt%	1.47 ± 0.23	122.40 ± 2.16
PKBS-20	PEEK/BS 20 wt%	2.03 ± 0.35	94.90 ± 1.10
PKBS-30	PEEK/BS 30 wt%	2.36 ± 0.32	60.59 ± 0.52
PKLS-10	PEEK/LS 10 wt%	1.52 ± 0.24	98.52 ± 1.75
PKLS-20	PEEK/LS 20 wt%	2.13 ± 0.16	113.10 ± 1.33
PKLS-30	PEEK/LS 30 wt%	3.32 ± 0.22	117.54 ± 1.07

PEEK chains are more compatible with hydrophobic nano-SiO<sub>2</sub> particles compared to hydrophilic ones. This is a major problem in all nanocomposites, where nanoparticles, because of their high surface area, tend to create agglomerates [40]. This is more observable for PEEK/SiO<sub>2</sub> nanocomposites containing hydrophilic nano-SiO<sub>2</sub> particles in this study. Thus, the presence of these particles results in increased surface roughness, which is in good agreement with the SEM micrographs.

### 3.6. Contact Angle Measurement

The variation of contact angle against different type and contents of nano-SiO<sub>2</sub> in the nanocomposites is given in the Table 2. In case of PEEK/SiO<sub>2</sub> nanocomposites loaded with hydrophobic nano-SiO<sub>2</sub>, the addition of 10 wt% of the hydrophobic nano-SiO<sub>2</sub> increases the contact angle value by 30% compared to the pure PEEK. Nevertheless, higher contents (20 and 30 wt%) reveal a decline in the contact angle values. This may be due to the presence of an excess of hydrophobic nano-SiO<sub>2</sub> on the surface of the nanocomposites [20,37]. Regarding the PEEK/SiO<sub>2</sub> nanocomposites loaded with hydrophilic nano-SiO<sub>2</sub>, it can be observed that the contact angle increases with an increase in hydrophilic nano-SiO<sub>2</sub> content in the nanocomposites. The increase in contact angle value can be compared with the increase in surface roughness of the PEEK surface. It has been shown that the contact angle increases with the increase in the roughness of the surface. These results show that the addition of the nano-SiO<sub>2</sub> particles can alter the hydrophobic character of the pure PEEK matrix, and the contact angle can be changed markedly via changing the content of the additive.

### 3.7. Microhardness

The results of the microhardness test for the pure PEEK and PEEK/SiO<sub>2</sub> nanocomposites are presented in Figure 5. The microhardness values increase significantly ( $p < 0.05$ ) when low contents (10 and 20 wt%) of hydrophobic nano-SiO<sub>2</sub> were incorporated in the nanocomposite formulation. For example, the addition of 10 wt% hydrophobic nano-SiO<sub>2</sub> increased the microhardness value from 38 to 57 Kg/mm<sup>2</sup>, that is, 50% higher than pure PEEK. This result could be due to the homogeneity and uniformity of the particles' distribution which gives rise to good adhesion between the particles and the PEEK matrix. Additionally, a decrease in interparticle distance, as particle loading in the matrix increased, led to an increase in PEEK matrix tolerance to indentation. Nanoparticles in the matrix are more alike than microparticles in the matrix for a given volume fraction, so nanoparticles can resist the indentation in the matrix more strongly [45]. On the other hand, a further increase in the hydrophobic nano-SiO<sub>2</sub> content (30 wt%) showed a statistically insignificant decrease in the microhardness value ( $p > 0.05$ ). The reason for this behavior may be attributed to the agglomeration of the nanoparticles and the lack of uniform dispersion.

The same trend of microhardness values was also observed in the PEEK/SiO<sub>2</sub> nanocomposites filled with hydrophilic nano-SiO<sub>2</sub> particles. It is worth noting that nanocomposites filled with hydrophilic nano-SiO<sub>2</sub> particles had significantly lower microhardness values compared to those filled with hydrophobic nano-SiO<sub>2</sub> particles.

These results may be endorsed by the alteration in particle size compatibility of the fillers used. The hydrophobic nano-SiO<sub>2</sub> has a smaller particle size ( $14.5 \pm 5$  nm), better microhardness values compared to the hydrophilic nano-SiO<sub>2</sub> ( $29 \pm 4$  nm), and more level dispersal in the PEEK matrix, therefore changing orientation of the polymer chains. Consequently, this leads to increased surface free energy of the resulting nanocomposite. Indeed, the surface properties of this nano-SiO<sub>2</sub> make it more compatible with PEEK molecular chains, resulting in raised total and polar surface free energies as well as microhardness [46].

Likewise, in similar research using SiO<sub>2</sub> nanoparticles with sizes ranging from 15 to 30 nm, the composites with finer nanoparticles witnessed a significant and linear increase in hardness, even at the maximum SiO<sub>2</sub> content of 10% by weight. The finer 15 nm particles are more evenly distributed, resulting in a continuously increasing hardness [47].

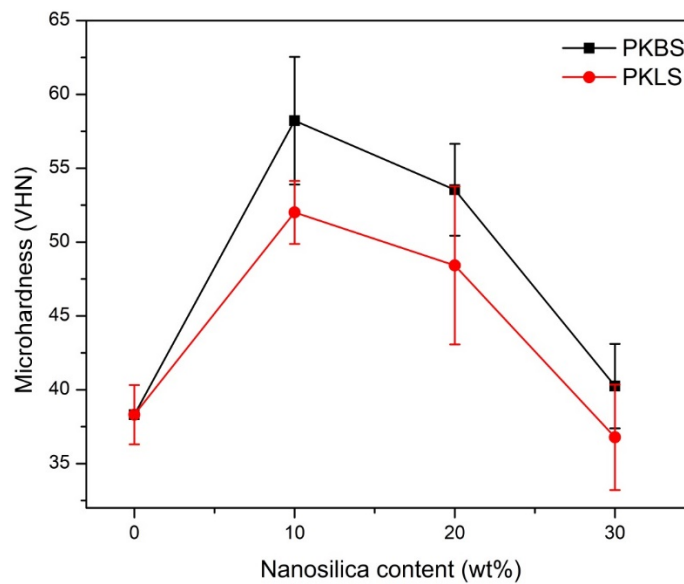


**Figure 5.** Mean value and standard deviations (mean  $\pm$  SD) of microhardness for the PEEK/SiO<sub>2</sub> nanocomposites as a function of the nano-SiO<sub>2</sub> content. ( $n = 7$ ).

### 3.8. Mechanical Properties

The compression elastic modulus and flexural strength of PEEK and its nanocomposites, fabricated by adding different contents of hydrophobic nano-SiO<sub>2</sub> and hydrophilic nano-SiO<sub>2</sub>, respectively, are shown in Figures 6 and 7. The addition of 10 wt% hydrophobic nano-SiO<sub>2</sub> showed a statistically significant increase in the compression elastic modulus by 40% compared to pure PEEK. However, there was a significant decrease by 5% and 65% in compression elastic modulus upon addition of 20 and 30 wt% hydrophobic nano-SiO<sub>2</sub>, respectively, compared to pure PEEK.

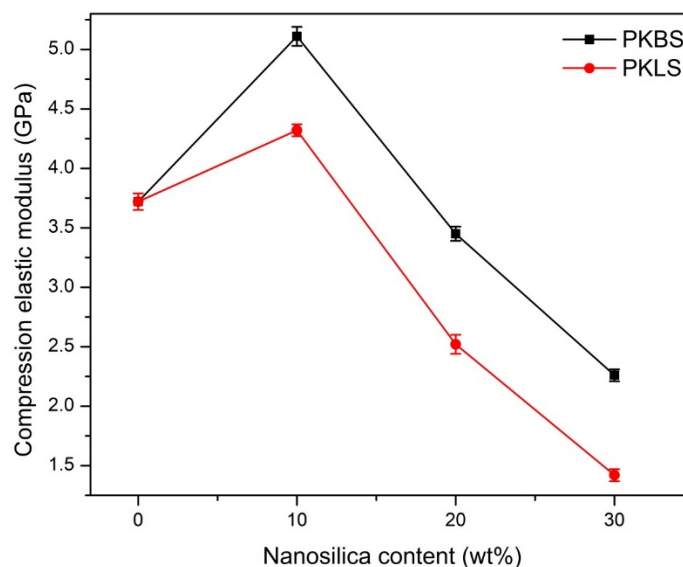


**Figure 6.** Mean value and standard deviations (mean  $\pm$  SD) of elastic compression modulus for the PEEK/SiO<sub>2</sub> nanocomposites as a function of the nano-SiO<sub>2</sub> content. ( $n = 7$ ).

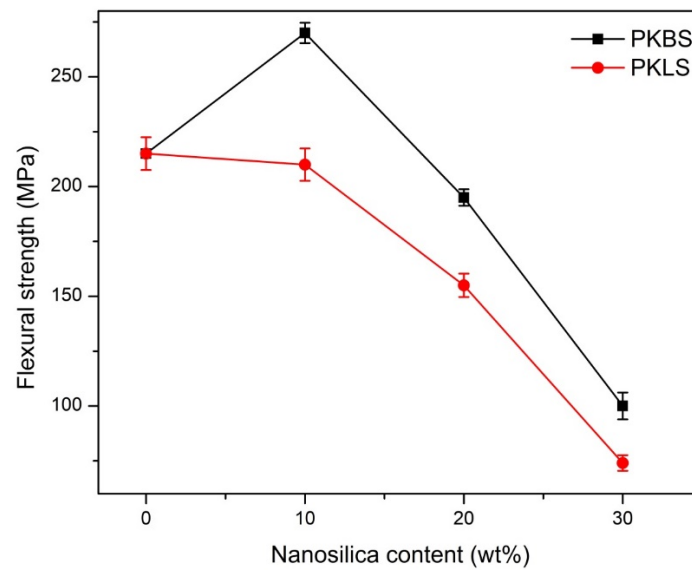


**Figure 7.** Mean value and standard deviations (mean  $\pm$  SD) of flexural strength for the PEEK/SiO<sub>2</sub> nanocomposites as a function of the nano-SiO<sub>2</sub> content. ( $n = 7$ ).

As for the nanocomposites loaded with hydrophilic nano-SiO<sub>2</sub>, the same pattern was observed. The compression elastic modulus was significantly enhanced by 25.3% compared to pure PEEK in the 10 wt% nanocomposite. Nevertheless, there was a significant decrease by 34.1% and 124.1% in the compression elastic modulus in 20 and 30 wt% nanocomposite, respectively. The measured elastic modulus data of nanocomposites filled with hydrophobic nano-SiO<sub>2</sub> appears significantly higher than the that of nanocomposites loaded with hydrophilic nano-SiO<sub>2</sub>, suggesting the effective enhancement of the filled hydrophobic nano-SiO<sub>2</sub> particles.

Regarding the flexural strength, 10 wt% hydrophobic nano-SiO<sub>2</sub> filled PEEK nanocomposite showed a significant increase of 33.9%, compared to pure PEEK, the trend of the increasing hydrophobic nano-SiO<sub>2</sub> content until 20 wt%. However, there was a significant decrease by 37.5% and 116.5% in flexural strength for nanocomposites loaded with 20 and 30 wt% hydrophobic nano-SiO<sub>2</sub>, respectively.

As for the nanocomposites loaded with hydrophilic nano-SiO<sub>2</sub>, the flexural strength value decreased by 3.3% for 10 wt% nanocomposite compared to PEEK, but this decrease was found to be insignificant. However, there was a significant decrease of 12.7% and 191.79% in flexural strength nanocomposites loaded with 20 and 30 wt% hydrophilic nano-SiO<sub>2</sub>, respectively, compared to the pure PEEK. Comparing the PKBS group to their corresponding PKLS group, there was a significant increase in flexural strength between PKBS-10 and PKLS-10. Moreover, the flexural strength values of the hydrophobic nano-SiO<sub>2</sub>-filled PEEK nanocomposites are statistically significantly higher than those of the hydrophilic nano-SiO<sub>2</sub>.

In general, it has already been documented that adding fillers to PEEK will improve its mechanical properties [48,49], while the addition of 30 wt% of nano-SiO<sub>2</sub> particles significantly decreased the mechanical properties. The incorporation of 30% vol of calcium silicate into PEEK resulted in a decrease of 20.84% in bending strength, according to a previously reported data [50].

The polarity imbalance between some of the hydrophilic nano-particle surfaces and the PEEK matrices, which resulted in poor dispersion of the nano-particles, could explain the higher elastic modulus of the hydrophobic nano-SiO<sub>2</sub> filled groups over their respective hydrophilic nano-SiO<sub>2</sub> filled groups [51]. Accordingly, the hydrophobic nano-SiO<sub>2</sub> particles disperse better in the PEEK matrix because of the matching polarity.

#### 4. Conclusions

The outcomes of the current research suggested that the addition of 10% hydrophobic nano-SiO<sub>2</sub> to the PEEK polymer matrix resulted in an improvement of the elastic modulus, flexural strength, and microhardness. Despite the high mechanical properties of the 10% hydrophilic nano-SiO<sub>2</sub> filled PEEK nanocomposite, compared to the pure PEEK, it is still significantly lower than the same weight percentage of hydrophobic nano-SiO<sub>2</sub>-filled PEEK nanocomposite. The incorporation of nano-SiO<sub>2</sub> fillers in a higher weight percentage (20% and 30%) significantly damages the mechanical characteristics of the resultant nanocomposites. As a result of the findings, treated PEEK/SiO<sub>2</sub> nanocomposites based on 10% hydrophobic nano-SiO<sub>2</sub> might be ideal for prosthodontics and restorative dentistry. Hence, it can be considered a promising potential alternative to metals such as titanium and zirconium due to its biochemical composition and high-quality mechanical properties. Despite being widely used as a progenitor material in the spinal column, orthopedics, and sports medicine, it has yet to reach critical mass in dental practice. However, further long-term clinical research into PEEK polymer as a substitute material for conventional metals is necessary.

**Author Contributions:** Conceptualization, A.A.E.-F.; Formal analysis, H.Y.; Investigation, A.A.E.-F.; Methodology, H.Y.; Software, H.Y.; Supervision, A.A.E.-F., M.A.H.G., R.A., S.K.; Writing—original draft, A.A.E.-F.; Writing—review & editing, S.K. All authors have read and agreed to the published version of the manuscript.

**Funding:** This research received no external funding.

**Institutional Review Board Statement:** Not applicable.

**Informed Consent Statement:** Not applicable.

**Data Availability Statement:** Not applicable.

**Conflicts of Interest:** The authors declare no conflict of interest.

#### References

1. Mehra, M.; Vahidi, F.; Berg, R.W. A complete denture impression technique survey of postdoctoral prosthodontic programs in the United States. *J. Prosthodont.* **2014**, *23*, 320–327. [[CrossRef](#)]
2. Saavedra, G.; Valandro, L.F.; Leite, F.P.P.; Amaral, R.; Özcan, M.; Bottino, M.A.; Kimpara, E.T. Bond strength of acrylic teeth to denture base resin after various surface conditioning methods before and after thermocycling. *Int. J. Prosthodont.* **2007**, *20*, 199–201.
3. Fischer, N.G.; Münchow, E.A.; Tamerler, C.; Bottino, M.C.; Aparicio, C. Harnessing biomolecules for bioinspired dental biomaterials. *J. Mater. Chem. B* **2020**, *8*, 8713–8747. [[CrossRef](#)] [[PubMed](#)]
4. Ferrando-Magraner, E.; Bellot-Arcís, C.; Paredes-Gallardo, V.; Almerich-Silla, J.M.; García-Sanz, V.; Fernández-Alonso, M. Antibacterial properties of nanoparticles in dental restorative materials. A systematic review and meta-analysis. *Medicina* **2020**, *56*, 55. [[CrossRef](#)] [[PubMed](#)]
5. Komabayashi, T.; Colmenar, D.; Cvach, N.; Bhat, A.; Primus, C.; Imai, Y. Comprehensive review of current endodontic sealers. *Dent. Mater. J.* **2020**, *39*, 703–720. [[CrossRef](#)]
6. Galante, R.; Figueiredo-Pina, C.G.; Serro, A.P. Additive manufacturing of ceramics for dental applications: A review. *Dent. Mater.* **2019**, *35*, 825–846. [[CrossRef](#)]
7. Chen, H.; Wang, R.; Zhang, J.; Hua, H.; Zhu, M. Synthesis of core-shell structured ZnO@m-SiO<sub>2</sub> with excellent reinforcing effect and antimicrobial activity for dental resin composites. *Dent. Mater.* **2018**, *34*, 1846–1855. [[CrossRef](#)] [[PubMed](#)]
8. Liu, X.; Gan, K.; Liu, H.; Song, X.; Chen, T.; Liu, C. Antibacterial properties of nano-silver coated PEEK prepared through magnetron sputtering. *Dent. Mater.* **2017**, *33*, e348–e360. [[CrossRef](#)]
9. Hanafy, R.A.; Mostafa, D.; Abd El-Fattah, A.; Kandil, S. Biomimetic chitosan against bioinspired nanohydroxyapatite for repairing enamel surfaces. *Bioinspired Biomim. Nanobiomater.* **2019**, *9*, 85–94. [[CrossRef](#)]
10. Alghazzawi, T.F. The effect of extended aging on the optical properties of different zirconia materials. *J. Prosthodont. Res.* **2017**, *61*, 305–314. [[CrossRef](#)] [[PubMed](#)]
11. Fernandez, C.C.; Sokolonski, A.R.; Fonseca, M.S.; Stanicic, D.; Araújo, D.B.; Azevedo, V.; Portela, R.D.; Tasic, L. Applications of Silver Nanoparticles in Dentistry: Advances and Technological Innovation. *Int. J. Mol. Sci.* **2021**, *22*, 2485. [[CrossRef](#)]
12. Liu, F.; Hong, T.; Xie, J.; Zhan, X.; Wang, Y. Application of Reactive Oxygen Species-Based Nanomaterials in Dentistry: A Review. *Crystals* **2021**, *11*, 266. [[CrossRef](#)]

13. Balbaa, A.O.; El-Fattah, A.A.; Awad, N.M.; Abdellatif, A. Effects of nanoscale electric fields on the histology of liver cell dysplasia. *Nanomedicine* **2019**, *14*, 515–528. [[CrossRef](#)] [[PubMed](#)]
14. Abd El-Fattah, A.; Nageeb Hassan, M.; Rashad, A.; Marei, M.; Kandil, S. Viscoelasticity, mechanical properties, and in vivo biocompatibility of injectable polyvinyl alcohol/bioactive glass composite hydrogels as potential bone tissue scaffolds. *Int. J. Polym. Anal. Charact.* **2020**, *25*, 362–373. [[CrossRef](#)]
15. Abd El-Fattah, A.; Mansour, A. Viscoelasticity, mechanical properties, and in vitro biodegradation of injectable chitosan-poly (3-hydroxybutyrate-co-3-hydroxyvalerate)/nanohydroxyapatite composite hydrogel. *Bull. Mater. Sci.* **2018**, *41*, 1–10. [[CrossRef](#)]
16. El-Fattah, A.A.; El Demerdash, A.G.M.; Alim Sadik, W.A.; Bedir, A. The effect of sugarcane bagasse fiber on the properties of recycled high density polyethylene. *J. Compos. Mater.* **2015**, *49*, 3251–3262. [[CrossRef](#)]
17. Parvinzadeh, M.; Moradian, S.; Rashidi, A.; Yazdanshenas, M.-E. Surface characterization of polyethylene terephthalate/silica nanocomposites. *Appl. Surf. Sci.* **2010**, *256*, 2792–2802. [[CrossRef](#)]
18. Zhong, F.; Xie, P.; Hou, R.; Niu, W.; Huang, J.; Hu, F.; Zheng, G.; Liu, H.; Qu, T.; Zhu, Y. Improved performance of sulfonated poly ether ether ketone/three-dimensional hierarchical molybdenum disulfide nanoflower composite proton exchange membrane for fuel cells. *J. Mater. Sci.* **2021**, *56*, 6531–6548. [[CrossRef](#)]
19. Dunlop, M.J.; Bissessur, R. Nanocomposites based on graphene analogous materials and conducting polymers: A review. *J. Mater. Sci.* **2020**, *55*, 6721–6753. [[CrossRef](#)]
20. Basgul, C.; Yu, T.; MacDonald, D.W.; Siskey, R.; Marcolongo, M.; Kurtz, S.M. Structure–property relationships for 3D-printed PEEK intervertebral lumbar cages produced using fused filament fabrication. *J. Mater. Res.* **2018**, *33*, 2040–2051. [[CrossRef](#)]
21. Wang, Y.; Shen, J.; Yan, M.; Tian, X. Poly ether ether ketone and its composite powder prepared by thermally induced phase separation for high temperature selective laser sintering. *Mater. Des.* **2021**, *201*, 109510. [[CrossRef](#)]
22. Akhtar, F.H.; Abdulhamid, M.A.; Vovusha, H.; Ng, K.C.; Schwingenschlög, U.; Szekely, G. Defining sulfonation limits of poly (ether-ether-ketone) for energy-efficient dehumidification. *J. Mater. Chem. A* **2021**, *9*, 17740–17748. [[CrossRef](#)]
23. Abdulhamid, M.A.; Park, S.H.; Vovusha, H.; Akhtar, F.H.; Ng, K.C.; Schwingenschlög, U.; Szekely, G. Molecular engineering of high-performance nanofiltration membranes from intrinsically microporous poly (ether-ether-ketone). *J. Mater. Chem. A* **2020**, *8*, 24445–24454. [[CrossRef](#)]
24. Yogarathinam, L.T.; Jaafar, J.; Ismail, A.F.; Goh, P.S.; Gangasalam, A.; Hanifah, M.F.R.; Wong, K.C.; Subramaniam, M.N.; Peter, J. Functionalized boron nitride embedded sulfonated poly (ether ether ketone) proton exchange membrane for direct methanol fuel cell applications. *J. Environ. Chem. Eng.* **2021**, *9*, 105876. [[CrossRef](#)]
25. Hao, L.; Hu, Y.; Zhang, Y.; Wei, W.; Hou, X.; Guo, Y.; Hu, X.; Jiang, D. Enhancing the mechanical performance of poly (ether ether ketone)/zinc oxide nanocomposites to provide promising biomaterials for trauma and orthopedic implants. *RSC Adv.* **2018**, *8*, 27304–27317. [[CrossRef](#)]
26. Santing, H.J.; Meijer, H.J.; Raghoobar, G.M.; Özcan, M. Fracture strength and failure mode of maxillary implant-supported provisional single crowns: A comparison of composite resin crowns fabricated directly over PEEK abutments and solid titanium abutments. *Clin. Implant. Dent. Relat. Res.* **2012**, *14*, 882–889. [[CrossRef](#)] [[PubMed](#)]
27. Lee, W.T.; Koak, J.Y.; Lim, Y.J.; Kim, S.K.; Kwon, H.B.; Kim, M.J. Stress shielding and fatigue limits of poly-ether-ether-ketone dental implants. *J. Biomed. Mater. Res. Part B Appl. Biomater.* **2012**, *100*, 1044–1052. [[CrossRef](#)] [[PubMed](#)]
28. Mishra, S.; Chowdhary, R. PEEK materials as an alternative to titanium in dental implants: A systematic review. *Clin. Implant. Dent. Relat. Res.* **2019**, *21*, 208–222. [[CrossRef](#)] [[PubMed](#)]
29. Kurtz, S.M.; Devine, J.N. PEEK biomaterials in trauma, orthopedic, and spinal implants. *Biomaterials* **2007**, *28*, 4845–4869. [[CrossRef](#)] [[PubMed](#)]
30. Díez-Pascual, A.M.; Díez-Vicente, A.L. Nano-TiO<sub>2</sub> reinforced PEEK/PEI blends as biomaterials for load-bearing implant applications. *ACS Appl. Mater. Interfaces* **2015**, *7*, 5561–5573. [[CrossRef](#)]
31. Schmidlin, P.R.; Stawarczyk, B.; Wieland, M.; Attin, T.; Hämmerle, C.H.; Fischer, J. Effect of different surface pre-treatments and luting materials on shear bond strength to PEEK. *Dent. Mater.* **2010**, *26*, 553–559. [[CrossRef](#)]
32. Lai, Y.-H.; Kuo, M.; Huang, J.; Chen, M. On the PEEK composites reinforced by surface-modified nano-silica. *Mater. Sci. Eng. A* **2007**, *458*, 158–169. [[CrossRef](#)]
33. Lümkemann, N.; Eichberger, M.; Stawarczyk, B. Bonding to different PEEK compositions: The impact of dental light curing units. *Materials* **2017**, *10*, 67. [[CrossRef](#)]
34. Silthampitag, P.; Chaijareenont, P.; Tattakorn, K.; Banjongprasert, C.; Takahashi, H.; Arksornnukit, M. Effect of surface pretreatments on resin composite bonding to PEEK. *Dent. Mater. J.* **2016**, *35*, 668–674. [[CrossRef](#)] [[PubMed](#)]
35. Sproesser, O.; Schmidlin, P.R.; Uhrenbacher, J.; Roos, M.; Gernet, W.; Stawarczyk, B. Effect of sulfuric acid etching of polyetheretherketone on the shear bond strength to resin cements. *J. Adhes. Dent.* **2014**, *16*, 465–472.
36. Zhang, M.; Matinlinna, J.P. E-glass fiber reinforced composites in dental applications. *Silicon* **2012**, *4*, 73–78. [[CrossRef](#)]
37. Hedayati, M.; Salehi, M.; Bagheri, R.; Panjepour, M.; Maghazan, A. Ball milling preparation and characterization of poly (ether ether ketone)/surface modified silica nanocomposite. *Powder Technol.* **2011**, *207*, 296–303. [[CrossRef](#)]
38. Dinari, M.; Soltani, R.; Mohammadnezhad, G. Kinetics and thermodynamic study on novel modified–mesoporous silica MCM-41/polymer matrix nanocomposites: Effective adsorbents for trace CrVI removal. *J. Chem. Eng. Data* **2017**, *62*, 2316–2329. [[CrossRef](#)]

39. Kuo, M.; Kuo, J.; Yang, M.; Huang, J. On the crystallization behavior of the nano-silica filled PEEK composites. *Mater. Chem. Phys.* **2010**, *123*, 471–480. [[CrossRef](#)]
40. Gashti, M.P.; Moradian, S.; Rashidi, A.; Yazdanshenas, M.-E. Dispersibility of hydrophilic and hydrophobic nano-silica particles in polyethylene terephthalate films: Evaluation of morphology and thermal properties. *Polym. Polym. Compos.* **2015**, *23*, 285–296. [[CrossRef](#)]
41. Bose, S.; Robertson, S.F.; Bandyopadhyay, A. Surface modification of biomaterials and biomedical devices using additive manufacturing. *Acta Biomater.* **2018**, *66*, 6–22. [[CrossRef](#)] [[PubMed](#)]
42. Mekuria, T.D.; Chunhong, Z.; Yingnan, L.; Fouad, D.E.D.; Lv, K.; Yang, M.; Zhou, Y. Surface modification of nano-silica by diisocyanates and their application in polyimide matrix for enhanced mechanical, thermal and water proof properties. *Mater. Chem. Phys.* **2019**, *225*, 358–364. [[CrossRef](#)]
43. Monich, P.R.; Berti, F.V.; Porto, L.M.; Henriques, B.; de Oliveira, A.P.N.; Fredel, M.C.; Souza, J.C. Physicochemical and biological assessment of PEEK composites embedding natural amorphous silica fibers for biomedical applications. *Mater. Sci. Eng. C* **2017**, *79*, 354–362. [[CrossRef](#)] [[PubMed](#)]
44. Tian, Q.; Zhang, C.; Tang, Y.; Liu, Y.; Niu, L.; Ding, T.; Li, X.; Zhang, Z. Preparation of hexamethyl disilazane-surface functionalized nano-silica by controlling surface chemistry and its “agglomeration-collapse” behavior in solution polymerized styrene butadiene rubber/butadiene rubber composites. *Compos. Sci. Technol.* **2021**, *201*, 108482. [[CrossRef](#)]
45. Tran, N.T.; Patterson, B.A.; Harris, D.E.; Napadensky, E.; Lenhart, J.L.; Knorr, D.B., Jr.; Bain, E.D. Influence of Interfacial Bonding on the Mechanical and Impact Properties Ring-Opening Metathesis Polymer (ROMP) Silica Composites. *ACS Appl. Mater. Interfaces* **2020**, *12*, 53342–53355. [[CrossRef](#)] [[PubMed](#)]
46. Gladson, T.F.; Ramesh, R.; Kavitha, C. Experimental investigation of mechanical, tribological and dielectric properties of alumina nano wire-reinforced PEEK/PTFE composites. *Mater. Res. Express* **2019**, *6*, 115327. [[CrossRef](#)]
47. Guo, L.; Zhang, G.; Wang, D.; Zhao, F.; Wang, T.; Wang, Q. Significance of combined functional nanoparticles for enhancing tribological performance of PEEK reinforced with carbon fibers. *Compos. Part A Appl. Sci. Manuf.* **2017**, *102*, 400–413. [[CrossRef](#)]
48. Duongthipthewa, A.; Su, Y.; Zhou, L. Electrical conductivity and mechanical property improvement by low-temperature carbon nanotube growth on carbon fiber fabric with nanofiller incorporation. *Compos. Part B Eng.* **2020**, *182*, 107581. [[CrossRef](#)]
49. Peng, C.; Li, X. The mechanical properties of PEEK/CF composites reinforced with ZrO<sub>2</sub> nanoparticles. *Mech. Compos. Mater.* **2014**, *49*, 679–684. [[CrossRef](#)]
50. Kim, I.Y.; Sugino, A.; Kikuta, K.; Ohtsuki, C.; Cho, S.B. Bioactive composites consisting of PEEK and calcium silicate powders. *J. Biomater. Appl.* **2009**, *24*, 105–118.
51. Mourdikoudis, S.; Pallares, R.M.; Thanh, N.T. Characterization techniques for nanoparticles: Comparison and complementarity upon studying nanoparticle properties. *Nanoscale* **2018**, *10*, 12871–12934. [[CrossRef](#)] [[PubMed](#)]